Article

Tuning the Valence of the Cerium Center in (Na)phthalocyaninato and Porphyrinato Cerium Double-Deckers by Changing the Nature of the Tetrapyrrole Ligands

Yongzhong Bian, Jianzhuang Jiang, Ye Tao, Michael T. M. Choi, Renjie Li, Anthony C. H. Ng, Peihua Zhu, Na Pan, Xuan Sun, Dennis P. Arnold, Zhong-Yuan Zhou, Hung-Wing Li, Thomas C. W. Mak, and Dennis K. P. Ng

J. Am. Chem. Soc., **2003**, 125 (40), 12257-12267• DOI: 10.1021/ja036017+ • Publication Date (Web): 13 September 2003

J|A|C|S
ARTICLES
Published on Web 09/13/2003

Tuning the Valence of the Cerium Center in (Na)phthalocyaninato and Porphyrinato Cerium Double-Deckers by Changing the Nature of the Tetrapyrrole Ligands

Yongzhong Bian,[†] Jianzhuang Jiang,*[,†] Ye Tao,[‡] Michael T. M. Choi,[§] Renjie Li,[†] Anthony C. H. Ng,[§] Peihua Zhu,[†] Na Pan,[†] Xuan Sun,[†] Dennis P. Arnold,[#] Zhong-Yuan Zhou,[§] Hung-Wing Li,[§] Thomas C. W. Mak,[§] and Dennis K. P. Ng*[,§]

Contribution from the Department of Chemistry, Shandong University, Jinan 250100, China, Laboratory of Synchrotron Radiation, Institute of High Energy Physics, Chinese Academy of Sciences, Beijing 100039, China, Department of Chemistry, The Chinese University of Hong Kong, Shatin, N.T., Hong Kong, China, and Synthesis and Molecular Recognition Program, School of Physical and Chemical Sciences, Queensland University of Technology, G.P.O. Box 2434, Brisbane, Qld. 4001, Australia

Received May 8, 2003; E-mail: jzjiang@sdu.edu.cn; dkpn@cuhk.edu.hk

Abstract: A series of 7 cerium double-decker complexes with various tetrapyrrole ligands including porphyrinates, phthalocyaninates, and 2,3-naphthalocyaninates have been prepared by previously described methodologies and characterized with elemental analysis and a range of spectroscopic methods. The molecular structures of two heteroleptic [(na)phthalocyaninato](porphyrinato) complexes have also been determined by X-ray diffraction analysis which exhibit a slightly distorted square antiprismatic geometry with two domed ligands. Having a range of tetrapyrrole ligands with very different electronic properties, these compounds have been systematically investigated for the effects of ligands on the valence of the cerium center. On the basis of the spectroscopic (UV−vis, near-IR, IR, and Raman), electrochemical, and structural data of these compounds and compared with those of the other rare earth(III) counterparts reported earlier, it has been found that the cerium center adopts an intermediate valence in these complexes. It assumes a virtually trivalent state in cerium bis(tetra-*tert*-butylnaphthalocyaninate) as a result of the two electron rich naphthalocyaninato ligands, which facilitate the delocalization of electron from the ligands to the metal center. For the rest of the cerium double-deckers, the cerium center is predominantly tetravalent. The valences (3.59−3.68) have been quantified according to their L_{III}-edge X-ray absorption near-edge structure (XANES) profiles.

Introduction

Sandwich-type rare earth complexes of tetrapyrrole derivatives, in particular phthalocyanines and porphyrins, have been investigated extensively since the first report of bis(phthalocyaninato) complexes [$M(Pc)_2$] in 1960s.[1] This class of complexes, with either a double- or triple-decker structure, usually exhibits strong $\pi-\pi$ interactions resulting in intriguing electronic and optical properties. These unique features together with other characteristics enable them to function as useful materials for a wide range of applications. Some recent papers have been published on their use as receptors for metal ions,[2] dicarboxylic acids,[3] and saccharides[4] utilizing positive homotropic allosterism, and molecular-based multibit information storage materials as a result of their rich redox properties.[5]

For the rare earth double-decker series, virtually all the neutral complexes can be formulated as [M^{III}(ring-1^{2-})(ring-$2^{\bullet-}$)], in which a trivalent metal center is sandwiched by a dianionic macrocycle and a radical anionic ligand, having different extent of electron delocalization. Among the whole rare earth series, cerium is the only exception. Having an electronic configuration

[†] Shandong University.
[‡] Institute of High Energy Physics, Chinese Academy of Sciences.
[§] The Chinese University of Hong Kong.
[#] Queensland University of Technology.

(1) (a) Kirin, I. S.; Moskalev, P. N.; Makashev, Y. A. *Russ. J. Inorg. Chem.* **1965**, *10*, 1065. (b) Ng, D. K. P.; Jiang, J. *Chem. Soc. Rev.* **1997**, *26*, 433. (c) Buchler, J. W.; Ng, D. K. P. In *The Porphyrin Handbook*; Kadish, K. M., Smith, K. M., Guilard, R., Eds.; Academic Press: San Diego, 2000; Vol. 3, pp 245−294. (d) Jiang, J.; Kasuga, K.; Arnold, D. P. In *Supramolecular Photo-sensitive and Electro-active Materials*; Nalwa, H. S., Ed.; Academic Press: New York, 2001, pp 113−210.

(2) (a) Ikeda, M.; Tanida, T.; Takeuchi, M.; Shinkai, S. *Org. Lett.* **2000**, *2*, 1803. (b) Robertson, A.; Ikeda, M.; Takeuchi, M.; Shinkai, S. *Bull. Chem. Soc. Jpn.* **2001**, *74*, 883. (c) Ikeda, M.; Takeuchi, M.; Shinkai, S.; Tani, F.; Naruta, Y.; Sakamoto, S.; Yamaguchi, K. *Chem. Eur. J.* **2002**, *8*, 5542.

(3) (a) Takeuchi, M.; Imada, T.; Shinkai, S. *Angew. Chem., Int. Ed.* **1998**, *37*, 2096. (b) Sugasaki, A.; Ikeda, M.; Takeuchi, M.; Robertson, A.; Shinkai, S. *J. Chem. Soc., Perkin Trans. 1* **1999**, 3259. (c) Takeuchi, M.; Ikeda, M.; Sugasaki, A.; Shinkai, S. *Acc. Chem. Res.* **2001**, *34*, 865.

(4) (a) Sugasaki, A.; Ikeda, M.; Takeuchi, M.; Shinkai, S. *Angew. Chem., Int. Ed.* **2000**, *39*, 3839. (b) Sugasaki, A.; Ikeda, M.; Takeuchi, M.; Koumoto, K.; Shinkai, S. *Tetrahedron* **2000**, *56*, 4717.

(5) (a) Li, J.; Gryko, D.; Dabke, R. B.; Diers, J. R.; Bocian, D. F.; Kuhr, W. G.; Lindsey, J. S. *J. Org. Chem.* **2000**, *65*, 7379. (b) Gryko, D.; Li, J.; Diers, J. R.; Roth, K. M.; Bocian, D. F.; Kuhr, W. G.; Lindsey, J. S. *J. Mater. Chem.* **2001**, *11*, 1162.

of [Xe]4f^{1}5d^{1}6s^2, this lanthanide may also utilize the electron in the extended 4f orbital in reactions leading to an additional +4 oxidation state. Tetravalent lanthanides are virtually confined to cerium, and to a much lesser extent praseodymium and terbium.[6] The unusual behavior of cerium can be attributed to the special stability of empty shell (4f^0). For all the bis(porphyrinato) complexes [Ce(Por)$_2$] and the mixed double-deckers [Ce(Pc)(Por)] reported so far,[7,8] it is believed that the cerium center is tetravalent and both tetrapyrrole rings are dianionic due to the absence of the characteristic spectral features for π radical anions (Pc$^{\bullet-}$ or Por$^{\bullet-}$) and the occurrence of relatively well-resolved ^{1}H NMR signals. Compared with the porphyrin analogues, bis(phthalocyaninato) cerium complexes have been little studied and the exact valence of the metal center remains elusive.[9−13] Homborg et al. reported some bis(phthalocyaninato) cerium double-deckers in which the cerium center was described as trivalent {e.g., [monocation][Ce^{III}(Pc^{2-})$_2$] and [Ce^{III}H(Pc^{2-})$_2$]}[9] or tetravalent {e.g., [Ce^{IV}(Pc^{2-})$_2$]}.[10] The crystal structure of [Ce(Pc)$_2$][BF$_4$]$_{0.33}$ was also determined which seemed to suggest an intermediate valence.[11] On the basis of the infrared and Ce 3d XPS spectroscopic data, Isago and Shimoda also suggested that the cerium center in [Ce(Pc)$_2$] is neither tri- nor tetra-valent and there is a partial delocalization of Pc π electron into a cerium 4f orbital.[12] We have recently reported the bis(naphthalocyaninato) cerium double-decker [Ce{Nc(*t*Bu)$_4$}$_2$],[7,13] the spectroscopic properties of which are similar to those of other rare earth analogues [M^{III}{Nc(*t*Bu)$_4$}$_2$] (M = La, Pr, Nd, Eu, Gd, Tb, Y, Er). This suggests the presence of a trivalent cerium center. To resolve and clarify this controversial issue, we have prepared a series of cerium double-deckers using a range of tetrapyrrole ligands with very different electronic properties (Figure 1), and systematically examined their electrochemical and spectroscopic properties, including the X-ray absorption near-edge structure (XANES) of the cerium center. The results reported herein demonstrate that the valent state of the cerium center varies from III to IV depending on the electronic nature of the two tetrapyrrole ligands.

Results and Discussion

Synthesis of Cerium Double-Decker Complexes. The new homoleptic bis(phthalocyaninato) complex [Ce{Pc(OC$_{12}$H$_{25}$)$_8$}$_2$] (**1c**)[7] was prepared by treating [Ce(acac)$_3$]·*n*H$_2$O with 4,5-bis(dodecyloxy)phthalonitrile in the presence of 1,8-diazabicyclo[5.4.0]undec-7-ene (DBU) (Scheme 1a). This represents a general procedure which has been employed by us previously

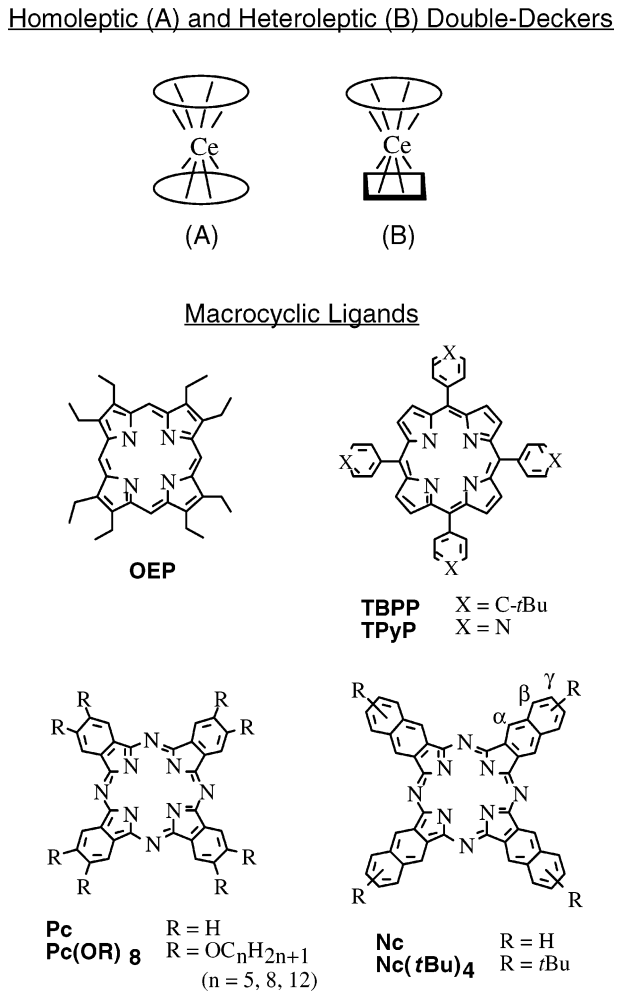

Figure 1. Schematic structures of cerium double-decker complexes with tetrapyrrole ligands.

Scheme 1. Synthesis of Cerium Double-Decker Complexes

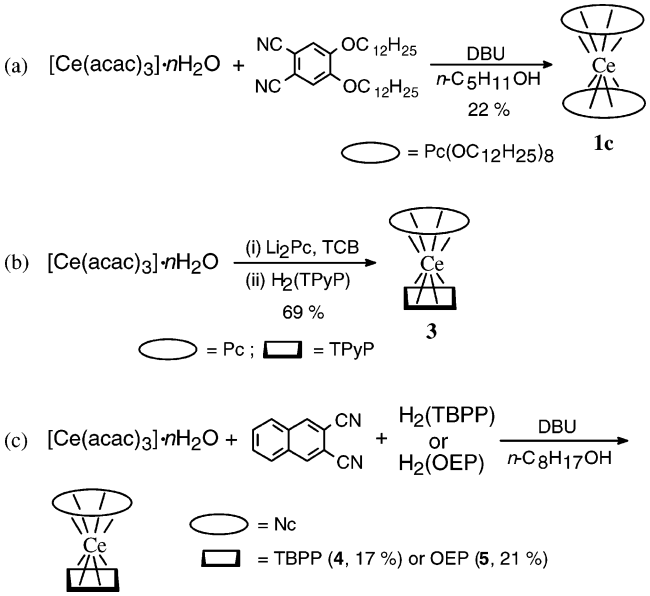

(6) Cotton, F. A.; Wilkinson, G.; Murillo, C. A.; Bochmann, M. *Advanced Inorganic Chemistry*, 6th ed.; Wiley: New York, 1999; pp 1109 and 1125−1127.
(7) Abbreviations used for tetrapyrrole derivatives: Nc = 2,3-naphthalocyaninate, Nc(*t*Bu)$_4$ = tetra(*tert*-butyl)-2,3-naphthalocyaninate, OEP = octaethylporphyrinate, Pc = phthalocyaninate, Pc(OR)$_8$ = 2, 3, 9, 10, 16, 17, 23, 24-octaalkoxyphthalocyaninate, Por = general porphyrinate, TBPP = *meso*-tetrakis(4-*tert*-butylphenyl)porphyrinate, TMPP = *meso*-tetrakis(4-methoxyphenyl)porphyrinate, TPP = *meso*-tetraphenylporphyrinate, TPyP = *meso*-tetra(4-pyridyl)porphyrinate.
(8) See for example: (a) Donohoe, R. J.; Duchowski, J. K.; Bocian, D. F. *J. Am. Chem. Soc.* **1988**, *110*, 6119. (b) Lachkar, M.; De Cian, A.; Fischer, J.; Weiss, R. *New J. Chem.* **1988**, *12*, 729. (c) Buchler, J. W.; De Cian, A.; Fischer, J.; Hammerschmitt, P.; Löffler, J.; Scharbert, B.; Weiss, R. *Chem. Ber.* **1989**, *122*, 2219. (d) Jiang, J.; Machida, K.; Yamamoto, E.; Adachi, G. *Chem. Lett.* **1991**, 2035. (e) Jiang, J.; Machida, K.; Adachi, G. *Bull. Chem. Soc. Jpn.* **1992**, *65*, 1990. (f) Tran-Thi, T.-H.; Mattioli, T. A.; Chabach, D.; De Cian, A.; Weiss, R. *J. Phys. Chem.* **1994**, *98*, 8279.
(9) (a) Haghighi, M. S.; Homborg, H. *Z. Naturforsch.* **1991**, *46b*, 1641. (b) Haghighi, M. S.; Homborg, H. *Z. Anorg. Allg. Chem.* **1994**, *620*, 1278. (c) Hückstädt, H.; Tuta*β*, A.; Göldner, M.; Cornelissen, U.; Homborg, H. *Z. Anorg. Allg. Chem.* **2001**, *627*, 485.
(10) Haghighi, M. S.; Teske, C. L.; Homborg, H. *Z. Anorg. Allg. Chem.* **1992**, *608*, 73.
(11) Ostendorp, G.; Rotter, H. W.; Homborg, H. *Z. Naturforsch.* **1996**, *51b*, 567.
(12) Isago, H.; Shimoda, M. *Chem. Lett.* **1992**, 147.
(13) Jiang, J.; Liu, W.; Poon, K.-W.; Du, D.; Arnold, D. P.; Ng, D. K. P. *Eur. J. Inorg. Chem.* **2000**, 205.

to prepare the pentyloxy [Ce{Pc(OC_5H_{11})$_8$}$_2$] (**1a**)[14] and octyloxy [Ce{Pc(OC_8H_{17})$_8$}$_2$] (**1b**) analogues,[15] together with other bis(phthalocyaninato) rare earth complexes.[15,16] The bis(naphthalocyaninato) analogues [M{Nc(*t*Bu)$_4$}$_2$] (M = La, Ce, Pr, Nd, Eu, Gd, Tb, Y, Er) have also been synthesized in a similar manner using 6-*tert*-butylnaphthalonitrile as the starting material.[13] The yield of the cerium double-decker [Ce{Nc(*t*Bu)$_4$}$_2$] (**2**) (71%) is much higher than those of the phthalocyanine counterparts **1a**−**1c** (9−49%) and follows the trend observed for the [M{Nc(*t*Bu)$_4$}$_2$] series, the yield of which decreases gradually with decreasing the size of the metal center.

The mixed ring double-decker [Ce(Pc)(TPyP)] (**3**)[7] was prepared by a stepwise procedure as shown in Scheme 1b. Reaction of [Ce(acac)$_3$]·*n*H_2O with Li_2Pc in 1,2,4-trichlorobenzene (TCB) followed by the addition of H_2(TPyP) led to **3** in 69% yield together with a substantial amount of the triple-deckers [Ce_2(Pc)(TPyP)$_2$] and [Ce_2(Pc)$_2$(TPyP)].[17] This procedure is one of the most common synthetic methods to prepare mixed double-deckers [M(Pc)(Por)].[1b−d] Weiss et al. have prepared the closely related double-deckers [Ce(Pc)(Por)] (Por = TPP, TMPP, OEP) and [Ce{Pc(OMe)$_8$}(TPP)] by reversing the order of addition of lithium phthalocyaninate and metal-free porphyrin.[7,8b]

By using the one-pot procedure developed recently by us,[18,19] the mixed double-deckers [Ce(Nc)(TBPP)] (**4**) and [Ce(Nc)-(OEP)] (**5**) were also synthesized.[7] As shown in Scheme 1c, treatment of [Ce(acac)$_3$]·*n*H_2O with the corresponding metal-free porphyrin and naphthalonitrile in the presence of DBU in *n*-octanol afforded these complexes in ca. 20% yield. It has been found that the yield of the double-deckers [M^{III}(Nc)(TBPP)] (M = Y, La−Tm except Ce and Pm) (from 73 to 29%)[18] and [M^{III}-(Nc)(OEP)] (M = Y, La−Lu except Ce and Pm) (from 45 to 21%)[19] decreases progressively with the size of the metal center as a result of an increase in axial compression of the two macrocyclic ligands. The yields of complexes **4** and **5**, which are lower than those expected for cerium(III) complexes, may indicate that the size of the cerium center in these double-deckers is actually smaller than a Ce^{III} ion.

Spectroscopic Properties. ^{1}H NMR Spectroscopy. The ^{1}H NMR spectra of **1a**−**1c** in $CDCl_3$ were very similar showing a slightly broad signal at δ 8.47−8.48 for the phthalocyanine ring protons, two multiplets at δ 4.77−4.86 and 4.44−4.53 due to the two sets of diastereotopic OCH_2 protons, along with other signals due to the alkyl chains. The naphthalocyanine analogue [Ce{Nc(*t*Bu)$_4$}$_2$] (**2**), however, did not give any signals in the aromatic region. The spectrum showed only several bands in the upfield region (δ 0.6−1.5), suggesting that the compound is strongly paramagnetic in nature.

The ^{1}H NMR spectrum of [Ce(Pc)(TPyP)] (**3**) in $CDCl_3$ (Figure 2a) showed two well-resolved AA′BB′ multiplets

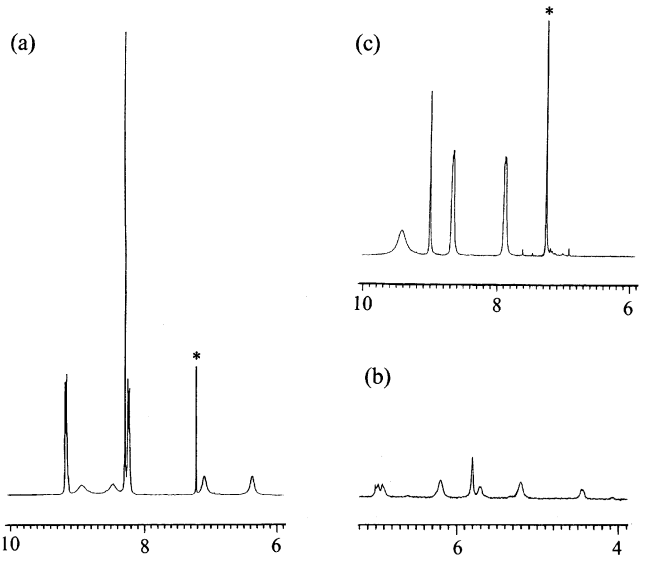

Figure 2. ^{1}H NMR spectra of (a) [Ce(Pc)(TPyP)] (**3**), (b) [Ce(Nc)(TBPP)] (**4**), and (c) [Ce(Nc)(OEP)] (**5**) in $CDCl_3$. The asterisk indicates residual solvent signal.

centered at δ 9.20 and 8.26 for the Pc ring protons. The β-protons of the TPyP ring resonated at δ 8.32 as a sharp singlet, while the four pyridyl protons' signals appeared as four broad bands at δ 8.98, 8.50, 7.13, and 6.40, as a result of restricted rotation along the C(*meso*)−C(*ipso*) bond. To further examine this dynamic process, a variable-temperature study was performed in toluene-d_8. Upon increasing the temperature, these four bands were broadened whereas the remaining signals did not change significantly. The two downfield pyridyl signals coalesced at 338 K and re-appeared as a broad band at ca. δ 8.8 at higher temperatures. The coalesced band for the remaining two pyridyl signals, however, was not observed which might be obscured by the strong residual solvent peaks. On the basis of these temperature-dependent NMR data, the free energy of activation $\Delta G^{\ddagger}$ for this rotational process was estimated to be 64.4 ± 0.5 kJ mol^{-1}.[20] The value is comparable with those of *para*-substituted tetraarylporphyrinato metal complexes which normally range from 60 to 80 kJ mol^{-1}.[21] Although this rotational process is well-known for sandwich-type complexes containing tetraarylporphyrinato ligands, the corresponding activation energies are not always given in the literature.[22]

Figure 2b shows part of the ^{1}H NMR spectrum of [Ce(Nc)-(TBPP)] (**4**) in $CDCl_3$. On the basis of the integration, the two broad bands at δ 6.10 and 5.15 can be assigned to the Nc's β and γ protons, the relatively sharp signal at δ 5.72 to the TBPP's β protons, and the four broad bands at δ 6.88, 6.81, 5.67, and 4.46 to the C_6H_4*t*Bu ring protons. Surprisingly, the spectrum does not show the signal due to the Nc's α protons. It is likely that the compound is slightly paramagnetic, leading to a broadening of signals, in particular for the Nc's α protons, which are nearest to the metal center. This is supported by the NMR data of [Ce(Nc)(OEP)] (**5**). As shown in Figure 2c, the signal

(14) Jiang, J.; Xie, J.; Ng, D. K. P.; Yan, Y. *Mol. Cryst. Liq. Cryst.* **1999**, *337*, 385.
(15) Liu, W.; Jiang, J.; Du, D.; Arnold, D. P. *Aust. J. Chem.* **2000**, *53*, 131. This compound was tentatively formulated as [CeH{Pc(OC_8H_{17})$_8$}$_2$] in this paper.
(16) (a) Jiang, J.; Liu, R. C. W.; Mak, T. C. W.; Chan, T. W. D.; Ng, D. K. P. *Polyhedron* **1997**, *16*, 515. (b) Jiang, J.; Xie, J.; Choi, M. T. M.; Yan, Y.; Sun, S.; Ng, D. K. P. *J. Porphyrins Phthalocyanines* **1999**, *3*, 322.
(17) The data of these compounds will be published elsewhere.
(18) Jiang, J.; Liu, W.; Cheng, K.-L.; Poon, K.-W.; Ng, D. K. P. *Eur. J. Inorg. Chem.* **2001**, 413.
(19) (a) Furuya, F.; Kobayashi, N.; Bian, Y.; Jiang, J. *Chem. Lett.* **2001**, 944. (b) Jiang, J.; Bian, Y.; Furuya, F.; Liu, W.; Choi, M. T. M.; Kobayashi, N.; Li, H.-W.; Yang, Q.; Mak, T. C. W.; Ng, D. K. P. *Chem. Eur. J.* **2001**, *7*, 5059 and a corrigendum appeared in **2002**, *8*, 2214.
(20) Friebolin, H. *Basic One- and Two-Dimensional NMR Spectroscopy*, 2nd ed.; VCH: Weinheim, 1993; pp 287−315.
(21) Medforth, C. J. In *The Porphyrin Handbook*; Kadish, K. M., Smith, K. M., Guilard, R., Eds.; Academic Press: San Diego, 2000; Vol. 5, pp 65−70 and references therein.
(22) (a) Buchler, J. W.; Eiermann, V.; Hanssum, H.; Heinz, G.; Rüterjans, H.; Schwarzkopt, M. *Chem. Ber.* **1994**, *127*, 589. (b) Davoras, E. M.; Spyroulias, G. A.; Eikros, E.; Coutsolelos, A. G. *Inorg. Chem.* **1994**, *33*, 3430.

Table 1. UV−Vis and Near-IR Spectroscopic Data for Double-Deckers **1c** and **3**−**5**

compd	solvent	λ_{max} (nm)
$[Ce\{Pc(OC_{12}H_{25})_8\}_2]$ (**1c**)	$CHCl_3$	357, ca. 500, 650, 686, 1650
$[Ce\{Pc(OC_{12}H_{25})_8\}_2]^+$	$CHCl_3$	361, 518, 648, 700, 1650
$[Ce\{Pc(OC_{12}H_{25})_8\}_2]^-$	$CHCl_3$/EtOH (1:1)	358, 647
[Ce(Pc)(TPyP)] (**3**)	$CHCl_3$	331, 398, 438, 465, 526, 633, 832
$[Ce(Pc)(TPyP)]^+$	$CHCl_3$	332, 399, 497, 635, 673, 692, 831
$[Ce(Pc)(TPyP)]^-$	$CHCl_3$/EtOH (1:1)	334, 382, 419, 483, 583, 626, 763
[Ce(Nc)(TBPP)] (**4**)	$CHCl_3$	323, 413, 479, 632, 685, 911
$[Ce(Nc)(TBPP)]^+$	$CHCl_3$	360, 408, 489, 621, 676, 922, 1088
$[Ce(Nc)(TBPP)]^-$	$CHCl_3$/EtOH (1:1)	330, 388, 428, 481, 638, 679, 840
[Ce(Nc)(OEP)] (**5**)	$CHCl_3$	324, 392, 467, 610, 660, 935
$[Ce(Nc)(OEP)]^+$	$CHCl_3$	322, 384, 452, 618, ca. 1200
$[Ce(Nc)(OEP)]^-$	$CHCl_3$/EtOH (1:1)	330, 406, 478, 601 (sh), 648, 741 (sh), 853

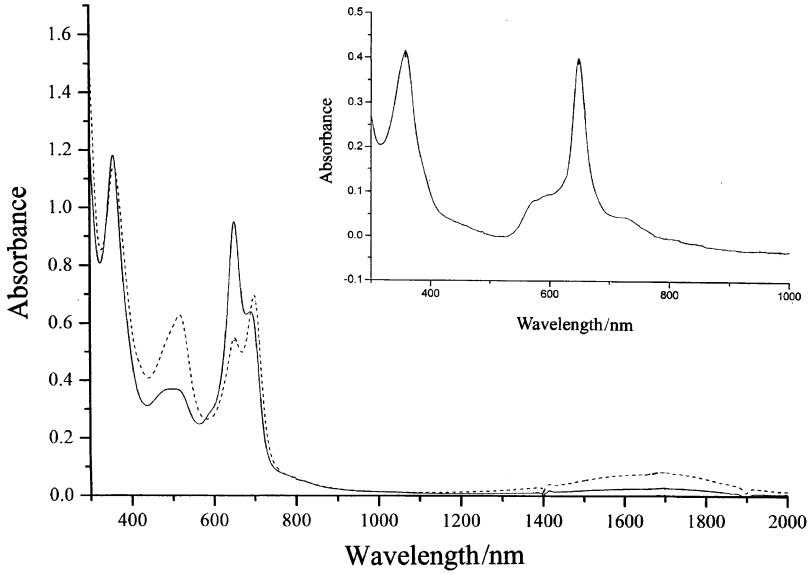

Figure 3. Electronic absorption spectra of $[Ce\{Pc(OC_{12}H_{25})_8\}_2]$ (**1c**) in $CHCl_3$ (——) and in the presence of excess iodine (- - -). The inset shows the spectrum of **1c** in $CHCl_3$ / EtOH (1:1) upon addition of hydrazine hydrate.

due to the Nc's α protons (δ 9.40) is also broad, while those of the Nc's β and γ protons (δ 8.63−8.66 and 7.86−7.89) are sharp and can be partially resolved. It is worth mentioning that these cerium compounds do not require the addition of reducing agent such as hydrazine hydrate or $NaBH_4$ to give satisfactory ^{1}H NMR spectra as in the cases of $[M^{III}(Nc)(TBPP)]$ (M = La, Nd, Sm, Eu)[18] and $[M^{III}(Nc)(OEP)]$ (M = Y, La, Eu, Lu).[19] This again shows the unique character of the cerium center in these complexes.

Electronic Absorption Spectroscopy. The electronic absorption data for the new double-deckers **1c** and **3**−**5** together with their monocations and anions are given in Table 1. The spectral data for **1a**−**1c** are virtually identical, so they are discussed using $[Ce\{Pc(OC_{12}H_{25})_8\}_2]$ (**1c**) as an example. As shown in Figure 3, the absorption spectrum of **1c** in $CHCl_3$ shows a typical phthalocyanine Soret band at 357 nm and two Q-bands at 650 and 686 nm. The splitting of Q-band has been observed in the spectra of $[M^{III}(Pc)_2]^-$[23] and $[M^{III}\{Pc(OC_8H_{17})_8\}_2]^-$[15] when the metal center is sufficiently small to induce a significant $\pi-\pi$ interaction between the two dianionic ligands. The separation of the two bands increases monotonically when the size of the metal center decreases. On the basis of the observation that the longer-wavelength Q-band just appears as a shoulder for the Nd complexes of the above two series and the fact that Ce^{III} (r = 1.143 Å) is larger than Nd^{III} (r = 1.109 Å),[24] the rather well-separated Q-bands for **1c** suggest that the actual size of the metal center in **1c** may be smaller than Ce^{III}.

The spectrum of **1c** also shows two broad bands at ca. 500 and 1650 nm, which are characteristic bands for bis(phthalocyaninato)lanthanide(III) complexes, arising from a phthalocyanine radical anion.[1b−d] As shown in Figure 3, these two bands increase in intensity upon oxidation with an excess of iodine, but vanish when hydrazine hydrate is added. The spectrum of reduced **1c** resembles those of $[La^{III}(Pc)_2]^-$[23] and $[La^{III}\{Pc(OC_8H_{17})_8\}_2]^-$,[15] showing a single Q-band at 647 nm. Compound **1c** thus exhibits the spectral features of both $[Ce^{IV}(ring^{2-})_2]$ and $[Ce^{III}(ring^{2-})(ring^{\bullet-})]$ [ring = $Pc(OC_{12}H_{25})_8$]. Upon reduction, the compound possesses the character of $[Ce^{III}(ring^{2-})_2]^-$. These spectral data suggest that the cerium center in **1a**−**1c** adopts an intermediate valence between III and IV. Due to their fairly well-resolved ^{1}H NMR spectra, it is believed that the cerium center is predominantly tetravalent in **1a**−**1c** with a partial delocalization of electron from a phthalocyanine π orbital to a metal-based orbital. It is worth noting that the two characteristic π radical bands do not appear in the spectrum of the unsubstituted analogue $[Ce(Pc)_2]$.[12] It is likely that the electron donating alkoxy substituents increase

(23) Iwase, A.; Harnoode, C.; Kameda, Y. *J. Alloys Compd.* **1993**, *192*, 280.

(24) Shannon, R. D. *Acta Crystallogr. Sect. A* **1976**, *32*, 751; the effective ionic radii of the octacoordinate metal ions were taken.

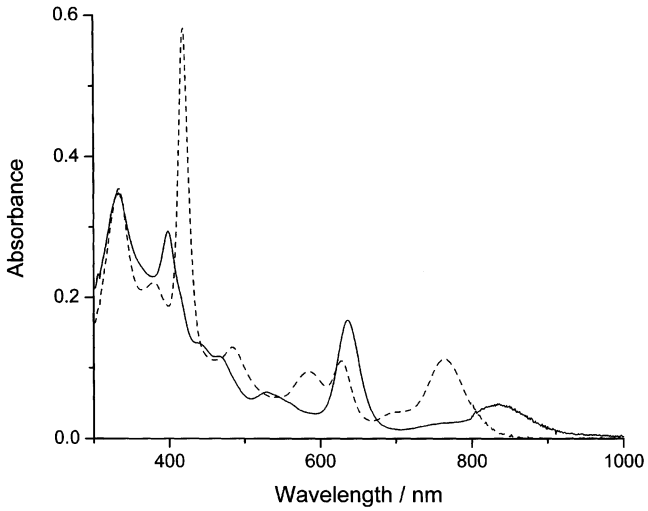

Figure 4. Electronic absorption spectra of [Ce(Pc)(TPyP)] (**3**) in $CHCl_3$ (——) and in $CHCl_3$/EtOH (1:1) in the presence of hydrazine hydrate (- - -).

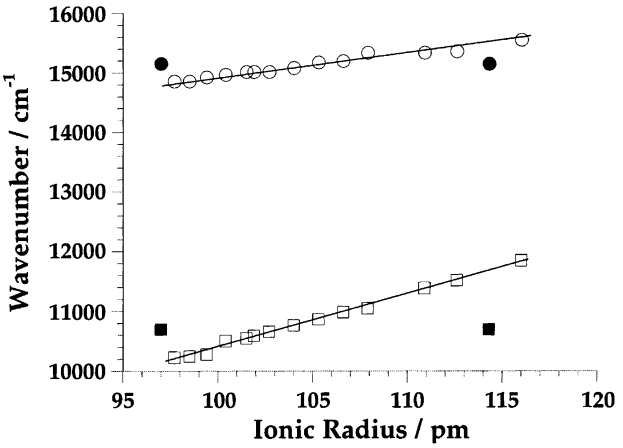

Figure 5. Wavenumbers of the two lowest-energy absorption bands of $[M^{III}(Nc)(OEP)]^-$ (M = Y, La−Lu except Ce and Pm) as a function of the ionic radius of the metal center.[24] The black circles and squares are generated by assuming a pure trivalent and tetravalent cerium center in [Ce(Nc)(OEP)] (**5**).

the electron density of the rings, facilitating the delocalization thereby enhancing the trivalent character of the cerium center.

The absorption spectrum of [Ce{Nc(*t*Bu)$_4$}$_2$] (**2**) is very different from those of the phthalocyanine counterparts **1a**−**1c**. As reported previously,[13] the spectra for the whole series of [M{Nc(*t*Bu)$_4$}$_2$] (M = La, Ce, Pr, Nd, Eu, Gd, Tb, Y, Er) are very similar, showing the spectral features of $[M^{III}(ring^{2-})(ring^{\bullet-})]$ [ring = Nc(*t*Bu)$_4$]. The positions of the π-radical anion band (593−648 nm), Q-band (767−799 nm), and the longest-wavelength near-IR band (1818−2346 nm) are all dependent linearly with the M^{III} ionic radii, including the data for the cerium compound **2** (see Figure S1 in the Supporting Information). This strongly suggests that the cerium center in **2**, like the other rare earth ions in this series, adopts a trivalent state. By a similar argument, the lower oxidation potential of Nc(*t*Bu)$_4$ (compared with the phthalocyanine analogues) facilitates the delocalization of electron from the ligands to the metal center, resulting in the formation of a trivalent cerium center and a π-radical anion.

Upon addition of $NaBH_4$ to solutions of the above series, the absorption spectra are remarkably changed and the resulting spectra can be attributed to the monoanions $[M^{III}(ring^{2-})_2]^-$ [ring = Nc(*t*Bu)$_4$], in which a trivalent metal center is sandwiched by two dianionic ligands.[13] Similarly to the phthalocyanine analogues,[15,23] the spectra display one to two Q-bands depending on the size of the metal center. The extent of Q-band splitting increases with decreasing the ionic radius of the M^{III} ions, reflecting the extent of $\pi-\pi$ interaction of the two naphthalocyanine rings. Again, the cerium complex anion $[Ce\{Nc(tBu)_4\}_2]^-$ strictly follows this relationship (see Figure S2 in the Supporting Information), suggesting that the cerium center still assumes a trivalent state in the anionic complex.

The absorption spectrum of [Ce(Pc)(TPyP)] (**3**) (Figure 4) resembles those of $[Ce^{IV}(Pc)(TPP)]$,[8b,8f] $[M^{IV}(Pc)(Por)]$ (M = Zr, Hf, Th, U),[25] and Li$[M^{III}(Pc)(TPyP)]$ (M = Eu, Gd),[26] in which both of the rings are regarded as dianionic. The spectrum shows strong Pc and TPyP Soret bands at 331 and 398 nm, respectively, and the Q-bands at 526, 633, and 832 nm. The lowest-energy Q-band is mainly contributed from the Pc Q-band. Compared with the spectra of Li$[M^{III}(Pc)(TPyP)]$ (M = Eu, Gd) in MeOH, the TPyP Soret band of **3** (398 nm) is significantly blue-shifted by 13−14 nm, whereas the longest-wavelength Q-band (832 nm) is red-shifted by 28−38 nm. The spectrum also shows two shoulders at 438 and 465 nm labeled as Q", which can be attributed to transitions from delocalized orbitals involving both macrocycles.[25] The spectrum of **3** is very different from those of $[M^{III}(Pc)(Por)]$.[26,27] Particularly, the characteristic near-IR absorption due to π radical anion was not detected. These data together with the well-resolved ^{1}H NMR spectrum strongly suggest that the cerium center in **3** is predominantly tetravalent.

The spectrum of **3**, after being treated with hydrazine hydrate (Figure 4), is very similar to that of $[NBu_4][Ce^{III}(Pc^{2-})(TPP^{2-})]$,[8f] suggesting that the first reduction is metal-based. This is corroborated with the observation that both the Pc and TPyP Soret bands, in particular the latter, are red-shifted upon reduction. This can be attributed to a lengthening of the ring-to-ring separation as a result of an increase in the metal size (from Ce^{IV} to Ce^{III}).[25b]

The spectral features of the Nc analogues **4** and **5** are similar to those of **3**, except that the Q-bands are significantly red-shifted due to the extended conjugation. In contrast to the other rare earth(III) counterparts,[18,19] near-IR absorptions over 1000 nm were not observed for **4** and **5**, showing that both of the ligands are essentially dianionic. The spectra, in fact, are similar to those of the anionic complexes $[M^{III}(Nc)(OEP)]^-$ (M = Y, La−Lu except Ce and Pm).[19] It has been found that there is a linear relationship between the positions of the two lowest-energy Q-bands and the size of the metal center for this series of complex anions. The data points generated by assuming a pure trivalent (r = 1.143 Å) and tetravalent (r = 0.970 Å) cerium center in **5** are clearly deviated from the straight lines (Figure 5). This again shows the unique nature of the cerium

(25) (a) Kadish, K. M.; Moninot, G.; Hu, Y.; Dubois, D.; Ibnlfassi, A.; Barbe, J.-M.; Guilard, R. *J. Am. Chem. Soc.* **1993**, *115*, 8153. (b) Guilard, R.; Barbe, J.-M.; Ibnlfassi, A.; Zrineh, A.; Adamian, V. A.; Kadish, K. M, *Inorg. Chem.* **1995**, *34*, 1472.
(26) Jiang, J.; Mak, T. C. W.; Ng, D. K. P. *Chem. Ber.* **1996**, *129*, 933.
(27) Chabach, D.; Tahiri, M.; De Cian, A.; Fischer, J.; Weiss, R.; El Malouli Bibout, M. *J. Am. Chem. Soc.* **1995**, *117*, 8548.

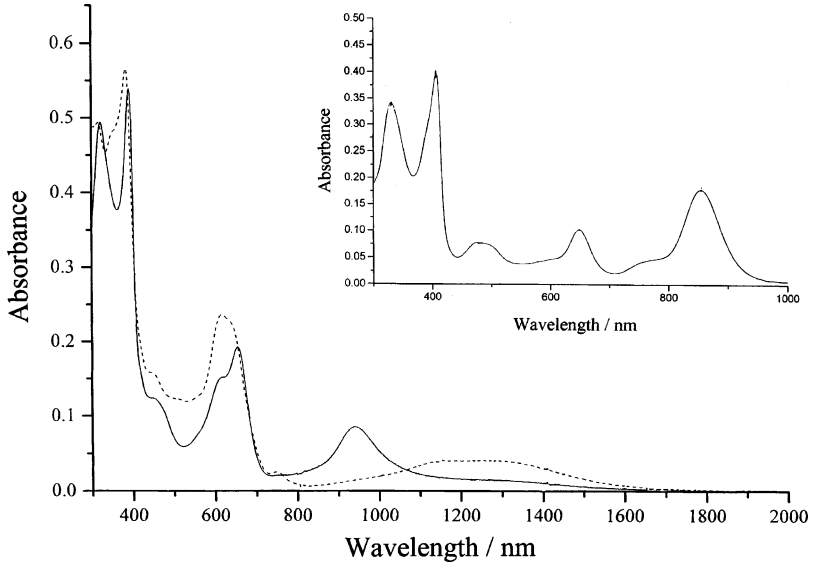

Figure 6. Electronic absorption spectra of [Ce(Nc)(OEP)] (**5**) in $CHCl_3$ (——) and in the presence of excess iodine (- - -). The inset shows the spectrum of **5** in $CHCl_3$/EtOH (1:1) upon addition of hydrazine hydrate.

center, which may adopt an intermediate valence between III and IV, lying closer to the tetravalent state. The results are in line with the XANES studies reported below.

Upon addition of hydrazine hydrate to a solution of **5**, the two Q-bands are shifted to the blue (Figure 6). Fitting the positions of these bands to the two straight lines in Figure 5 gives an ionic radius of ca. 1.14 Å, which is very close to the size of a Ce^{III} center. The results thus suggest that the reduction occurs preferentially at the metal center leading to the formula $[Ce^{III}(Nc^{2-})(OEP^{2-})]^-$. This is corroborated by the red-shifted Nc and OEP Soret bands in $[Ce(Nc)(OEP)]^-$, which indicate an increase in ring-to-ring separation when the cerium center changes from tetravalent to trivalent.[25b] Similar spectral changes were observed upon reduction of **4** (Table 1).

Oxidation of **5** with iodine slightly shifts the Soret bands and the Q-bands to the blue (Figure 6). The longest-wavelength Q-band at 935 nm disappears and a broad near-IR band centering at ca. 1200 nm emerges, indicating the presence of a π-radical anion. The spectrum is similar to those of $[M^{III}(Nc)(OEP)]$ (M = Ho−Lu), which also show one rather than two near-IR absorptions as the lighter lanthanide analogues (M = La−Dy except Ce and Pm) do.[19b] These observations suggest that the metal center in $[Ce(Nc)(OEP)]^+$ is smaller than Ce^{III}, and it is likely that the electron is removed from a ligand-based orbital and the metal center retains its predominant tetravalent state. A new near-IR band was also observed at 1088 nm upon oxidation of **4** with iodine.

IR Spectroscopy. The IR spectra of **1a**−**1c** showed a strong band at ca. 1380 cm^{-1}, which is a marker band for alkoxy substituted phthalocyanine dianions.[28] The intense characteristic phthalocyanine π-radical anion band at 1310−1320 cm^{-1} was not observed. These results provided further evidence for the predominant $[Ce^{IV}(ring^{2-})_2]$ [ring = $Pc(OC_nH_{2n+1})_8$] character in these complexes. In contrast, the naphthalocyanine analogue **2** gave a strong IR band at 1313 cm^{-1}, which can be assigned to $Nc(tBu)_4^{\bullet-}$, confirming a trivalent cerium center.[13,29]

The mixed ring complexes $[M^{III}(Pc)(Por)]$ (Por = TPP and its derivatives) usually show a strong IR band at 1310−1320 cm^{-1} assignable to the $Pc^{\bullet-}$ radical anion because of the lower oxidation potential of Pc compared with that of Por.[26−30] The IR spectrum of [Ce(Pc)(TPyP)] (**3**), however, showed a strong band at 1330 cm^{-1}, indicating that Pc^{2-} rather than $Pc^{\bullet-}$ is present in **3**[27] and the cerium center is therefore mainly tetravalent. Similarly, the IR spectra of the naphthalocyanine analogues **4** and **5** did not show the marker bands for $Nc^{\bullet-}$ (ca. 1320 cm^{-1}) and $TBPP^{\bullet-}$ (ca. 1280 cm^{-1}) or $OEP^{\bullet-}$ (ca. 1530 cm^{-1}). These spectral features are very different from those of the other rare earth(III) congeners, for which a strong $Nc^{\bullet-}$ marker band at 1319−1325 cm^{-1} (for the $[M^{III}(Nc)(TBPP)]$ series)[18] or both the $Nc^{\bullet-}$ and $OEP^{\bullet-}$ marker bands at 1315−1325 and 1510−1531 cm^{-1}, respectively (for the $[M^{III}(Nc)(OEP)]$ series)[19b] were observed. All of these results supported the tetravalent state of the cerium center in these complexes.

Raman Spectroscopy. In addition to the IR spectroscopy, Raman spectroscopy is another valuable tool for analyzing the extent of hole (de)localization in these sandwich-like complexes. By analyzing the Raman spectra of a vast number of phthalocyanine-containing sandwich complexes, it has been found that, upon excitation at 632.8 or 647.1 nm, the Raman band at ca. 1500 cm^{-1} is a characteristic band for the phthalocyanine dianions.[31] This vibrational band, which can be attributed to the coupled C═C and C═N stretches, shifts slightly to the higher energy side at ca. 1510−1520 cm^{-1} when one electron is removed from the macrocyclic rings forming π radical anions. The Raman spectra of $[Ce\{Pc(OC_8H_{17})_8\}_2]$ (**1b**) and [Ce(Pc)(TPyP)] (**3**), upon excitation at 632.8 nm, showed an intense band at 1500 and 1493 cm^{-1}, respectively, confirming the presence of phthalocyanine dianions in these complexes.

(28) (a) Jiang, J.; Arnold, D. P.; Yu, H. *Polyhedron* **1999**, *18*, 2129. (b) Lu, F.; Bao, M.; Ma, C.; Zhang, X.; Arnold, D. P.; Jiang, J. *Spectrochim. Acta A* **2003**, in press. (c) Bao, M.; Pan, P.; Ma, C.; Arnold, D. P.; Jiang, J. *Vibrational Spectrosc.* **2003**, *32*, 175.

(29) Sun, X.; Bao, M.; Pan, N.; Cui, X.; Arnold, D. P.; Jiang, J. *Aust. J. Chem.* **2002**, *55*, 587.

(30) Jiang, J.; Choi, M. T. M.; Law, W.-F.; Chen, J.; Ng, D. K. P. *Polyhedron* **1998**, *17*, 3903.

(31) (a) Jiang, J.; Rintoul, L.; Arnold, D. P. *Polyhedron* **2000**, *19*, 1381. (b) Jiang, J.; Cornelissen, U.; Arnold, D. P.; Sun, X.; Homborg, H. *Polyhedron* **2001**, *20*, 557.

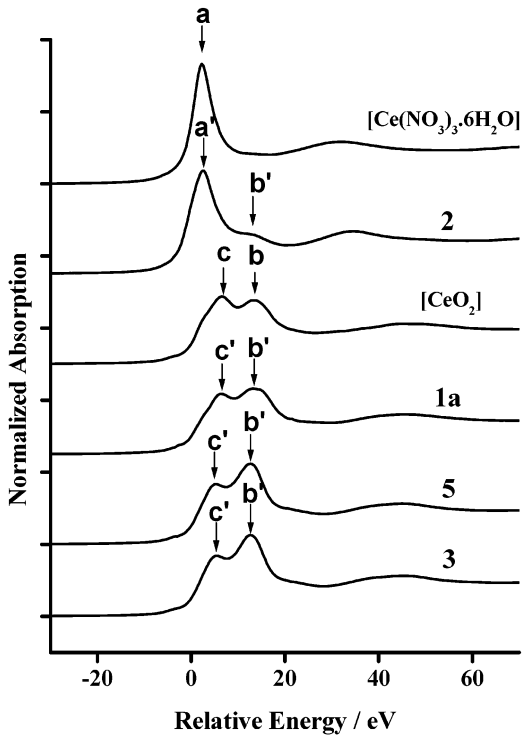

Figure 7. XANES spectra of selected cerium double-deckers and references.

Table 2. XANES Data for the Cerium Double-Deckers **1a**, **2**, **3**, and **5** and the References

compd	relative energy (eV)	
$[Ce(NO_3)_3 \cdot 6H_2O]$	2.27	
$[Ce\{Nc(t\text{Bu})_4\}_2]$ (**2**)	2.42	11.76
$[CeO_2]$	6.52	13.43
$[Ce\{Pc(OC_5H_{11})_8\}_2]$ (**1a**)	6.18	13.06
[Ce(Pc)(TPyP)] (**3**)	5.46	12.52
[Ce(Nc)(OEP)] (**5**)	5.38	12.68

The Raman data of [Ce(Nc)(TBPP)] (**4**) and [Ce(Nc)(OEP)] (**5**) are significantly different from those of their other rare earth-(III) counterparts, both under excitation at 632.8 and 785 nm.[32] The spectral properties of $[Ce\{Nc(t\text{Bu})_4\}_2]$ (**2**), however, closely resemble those of the other trivalent rare earth analogues.[33] A linear relationship has been found for some of the Raman bands of this series of complexes with the ionic radius of the metal center. The data for compound **2**, by assuming a pure trivalent state, fit reasonably well into these relationships.

XANES Spectroscopy. To reveal the valence of the cerium center in these complexes in a more quantitative manner, their XANES spectra were recorded. The spectra of **1a**, **2**, **3**, **5**, and the two references $[Ce(NO_3)_3 \cdot 6H_2O]$ and $[CeO_2]$ are shown in Figure 7 and the corresponding data are summarized in Table 2. It can be seen that the spectrum of $[Ce\{Nc(t\text{Bu})_4\}_2]$ (**2**) resembles that of the cerium(III) reference $[Ce(NO_3)_3 \cdot 6H_2O]$, but is remarkably different from those of the other double-deckers. It displays a single and intense edge resonance at 2.42 eV, labeled as a′, which is a typical feature observed in the L_{III}-edge XANES spectra of trivalent cerium compounds and can be attributed to the $2p \rightarrow 4f^1 5d$ dipole-allowed transition.[34] The peak is slightly broader than that of $[Ce(NO_3)_3 \cdot 6H_2O]$, having a tail labeled as b′ at 11.76 eV extending to the higher energy side. Because a related peak, labeled as b, was also observed in the spectrum of $[CeO_2]$, which can be attributed to the $2p \rightarrow 4f^0 5d$ transition in tetravalent cerium configuration, the appearance of b′ in the spectrum of **2** may indicate the component of tetravalent cerium in this compound. On the basis of the relative intensity of peaks a′ and b′, it is clear that compound **2** is largely trivalent which is in accord with all the spectroscopic data reported in previous sections.

The XANES spectra of $[Ce\{Pc(OC_5H_{11})_8\}_2]$ (**1a**), [Ce(Pc)-(TPyP)] (**3**), and [Ce(Nc)(OEP)] (**5**) are characterized by two strong resonance absorption peaks labeled as b′ and c′, which have counterparts in the spectrum of $[CeO_2]$ (Figure 7). There has been some controversy about the valent state of cerium in $[CeO_2]$. Now it is generally believed that cerium adopts an intermediate valence in the ground state due to the strong hybridization of the intrinsic tetravalent cerium 4f orbitals with the oxygen 2p orbitals.[35] In the XANES spectrum, the peak b is due to the $2p \rightarrow 4f^0 5d$ transition, whereas the peak c can be attributed to the transition from a cerium 2p orbital to the hybridization state consisting of cerium 4f orbitals and oxygen 2p orbitals. The relative intensity of these two signals reflects the weight of hybridization between the cerium center and the ligand. Accordingly, the peaks b′ and c′ of the double-deckers can be assigned in a similar manner. The peak c′ can therefore be ascribed to the transition from a cerium 2p orbital to the hybrid orbitals constructed from cerium 4f orbitals and the nitrogen-based orbitals. A close examination of the spectra reveals some differences between $[CeO_2]$ and the double-deckers **1a**, **3**, and **5**. First, the two signals for the double-deckers appear at the lower-energy side compared with those of $[CeO_2]$ (Table 2) as a result of different ligated atoms. Second, the peak b′ is more intense than peak c′ for the double-deckers, in particular compounds **3** and **5**, which have almost the same XANES profile. A reverse is seen in the spectrum of $[CeO_2]$, indicating the more profound hybridization and higher trivalent character in this compound.

To quantify the valence of these double-deckers, we subtracted a simple arctangent function from the L_{III}-edge XANES profile to simulate the atomic absorption jump, i.e., $2p_{3/2}$ to continuum transition, and then fitted the residue with three Lorentzian functions to model the two valent states and a pre-edge peak (see Figure S3 in the Supporting Information). The values were found to be 3.59 for $[Ce\{Pc(OC_5H_{11})_8\}_2]$ (**1a**) and 3.68 for [Ce(Pc)(TPyP)] (**3**) and [Ce(Nc)(OEP)] (**5**), which are slightly higher than that of $[CeO_2]$ (<3.50) reported earlier.[36] These results indicated the higher tetravalent character of **3** and **5**, which again is consistent with the other spectroscopic and electrochemical (as reported below) data.

Electrochemical Properties. The electrochemical properties of all the cerium double-deckers were investigated by cyclic

(32) (a) Bian, Y.; Rintoul, L.; Arnold, D. P.; Wang, R.; Jiang, J. *Vibrational Spectrosc.* **2003**, *31*, 173. (b) Sun, X.; Rintoul, L.; Bian, Y.; Arnold, D. P.; Wang, R.; Jiang, J. *J. Raman Spectrosc.* **2003**, *34*, 306.
(33) Pan, N.; Rintoul, L.; Arnold, D. P.; Jiang, J. *Polyhedron* **2002**, *21*, 1905.
(34) Zhang, J.; Wu, Z.; Liu, T.; Hu, T.; Wu, Z.; Ju, X. *J. Synchrotron Radiation* **2001**, *8*, 531.
(35) (a) Fujimori, A. *Phys. Rev. B* **1983**, *28*, 4489. (b) Kotani, A.; Ogasawara, H. *J. Elect. Spectrosc. Related Phenom.* **1992**, *60*, 257. (c) Soldatov, A. V.; Ivanchenko, T. S.; Dellalonga, S.; Kotani, A.; Iwamoto, Y.; Bianconi, A. *Phys. Rev. B* **1994**, *50*, 5074. (d) Antonio, M. R.; Soderholm, L. *Inorg. Chem.* **1994**, *33*, 5988.
(36) Bianconi, A.; Marcelli, A.; Dexpert, H.; Karnatak, R.; Kotani, A.; Jo, T.; Petiau, J. *Phys. Rev. B* **1987**, *35*, 806.

Table 3. Electrochemical Data for the Cerium Double-Deckers **1**−**5**[a]

compd	$E_{1/2}$ (oxd.4)	$E_{1/2}$ (oxd.3)	$E_{1/2}$ (oxd.2)	$E_{1/2}$ (oxd.1)	$E_{1/2}$ (red.1)	$E_{1/2}$ (red.2)	$E_{1/2}$ (red.3)	$E_{1/2}$ (red.4)
[Ce{Pc(OC_5H_{11})$_8$}$_2$] (**1a**)		+1.55	+0.74	+0.30	−0.18	−1.32	−1.69[b]	
[Ce{Pc(OC_8H_{17})$_8$}$_2$] (**1b**)			+0.74	+0.29	−0.21	−1.34	−1.68[b]	
[Ce{Pc($OC_{12}H_{25}$)$_8$}$_2$] (**1c**)		+1.57	+0.77	+0.31	−0.20	−1.33[b]	−1.63	
[Ce{Nc(*t*Bu)$_4$}$_2$] (**2**)	+1.54[b]	+1.36	+0.69	+0.17	−0.11	−1.20	−1.52	−1.88[b]
[Ce(Pc)(TPyP)] (**3**)		+1.72[b]	+1.26	+0.73	+0.10	−1.24	−1.56[b]	−1.85[b]
[Ce(Nc)(TBPP)] (**4**)	+1.69	+1.46	+0.84	+0.30	−0.07	−1.38	−1.80[b]	−1.93[b]
[Ce(Nc)(OEP)] (**5**)	+1.83[b]	+1.55	+0.71	+0.20	−0.19	−1.45	−1.88[b]	

[a] Recorded with [NBu_4][ClO_4] as electrolyte in CH_2Cl_2 (0.1 mol dm^{-3}) at ambient temperature. Potentials were obtained by cyclic voltammetry with a scan rate of 20 mV s^{-1} unless otherwise stated, and are expressed as half-wave potentials ($E_{1/2}$) in volts relative to SCE. [b] By differential pulse voltammetry with a scan rate of 10 mV s^{-1}.

voltammetry (CV) and differential pulse voltammetry (DPV) in CH_2Cl_2. The data are summarized in Table 3. All the cerium double-deckers exhibited a number of quasi-reversible or reversible one-electron redox processes {except the second oxidation process for [Ce{Nc(*t*Bu)$_4$}$_2$] (**2**) as reported below} depending on the nature of the tetrapyrrole rings.

The CV and DPV voltammograms of [Ce{Pc(OC_8H_{17})$_8$}$_2$] (**1b**) were different from those recorded previously.[37] Probably due to the higher concentration (by about two times at ca. 0.1 mol dm^{-3}), two additional one-electron reduction processes were clearly revealed this time. With reference to the data of its analogues [M^{III}{Pc(OC_8H_{17})$_8$}$_2$] (M = Y, La−Lu except Ce and Pm), the second and third reduction couples of **1b** at −1.34 and −1.68 V can be attributed to a successive addition of electrons to the ligand-based orbitals that are represented by the following redox states: [Ce{Pc(OC_8H_{17})$_8$}$_2$]$^-$/[Ce{Pc(OC_8H_{17})$_8$}$_2$]$^{2-}$ and [Ce{Pc(OC_8H_{17})$_8$}$_2$]$^{2-}$/[Ce{Pc(OC_8H_{17})$_8$}$_2$]$^{3-}$, respectively. In these redox states, the cerium center is believed to be trivalent because both these potentials follow the linear dependence of the second and third reduction potentials of the series [M^{III}{Pc(OC_8H_{17})$_8$}$_2$] on the size of the metal center.[37] The first reduction wave at −0.21 V is metal-centered and can be ascribed to [Ce^X{Pc(OC_8H_{17})$_8^{n-}$}$_2$]/[Ce^{III}{Pc(OC_8H_{17})$_8^{2-}$}$_2$]$^-$ couple, where the value of *X* lies between III and IV, and *n* is the formal charge of the ring to maintain the overall charge of the complex. The first and second oxidation processes at +0.29 and +0.74 V for **1b** involve a successive removal of electrons from the ligand-based HOMO and can be attributed to [Ce^X{Pc(OC_8H_{17})$_8$}$_2$]/[Ce^X{Pc(OC_8H_{17})$_8$}$_2$]$^+$ and [Ce^X{Pc(OC_8H_{17})$_8$}$_2$]$^+$/[Ce^X{Pc(OC_8H_{17})$_8$}$_2$]$^{2+}$ couples, respectively, in which the ligands also contain a fractional formal charge to maintain the overall charge of the complex. It is likely that the cerium ion in these redox states is not trivalent and may have the same formal charge as in the neutral complex **1b** because both these potentials deviate significantly from the linear relationship established between the potentials of corresponding redox processes (i.e., the first reduction and first oxidation) of [M^{III}{Pc(OC_8H_{17})$_8$}$_2$] and the rare earth ionic radii.[37] Compounds **1a** and **1c** behaved similarly except that one additional oxidation couple at +1.55 (for **1a**) or +1.57 V (for **1c**) was revealed for these compounds.

As shown in Figure 8, [Ce(Nc)(OEP)] (**5**) exhibits seven distinct single-electron redox processes. The second and third reduction couples at −1.45 and −1.88 V are ligand-based processes relating to the following redox states: [Ce(Nc)(OEP)]$^-$/[Ce(Nc)(OEP)]$^{2-}$ and [Ce(Nc)(OEP)]$^{2-}$/[Ce(Nc)(OEP)]$^{3-}$, respectively. The second reduction potential follows the trend observed for the series [M^{III}(Nc)(OEP)] (M ≠ Ce and Pm) (Figure 9),[19b] suggesting that the cerium center in these states is also trivalent. The anomalous first reduction wave at −0.19 V is thus metal-based and can be ascribed to [Ce^X(Nc)(OEP)]/[Ce^{III}(Nc^{2-})(OEP^{2-})]$^-$ couple, where X lies between III and IV. The four oxidation processes at +0.20, +0.71, +1.55,

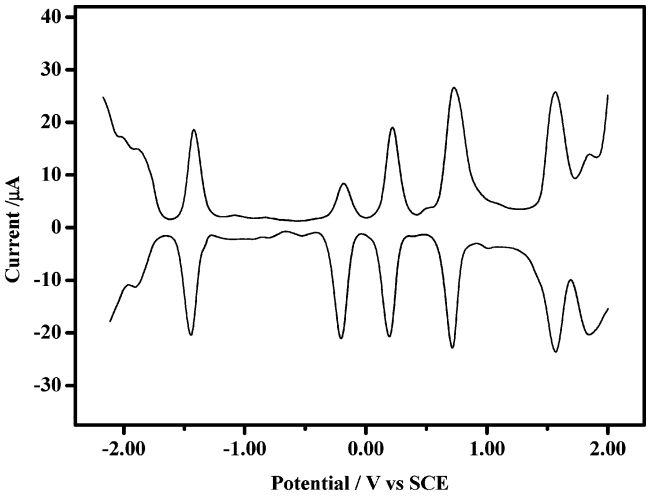

Figure 8. Differential pulse voltammogram of [Ce(Nc)(OEP)] (**5**) in CH_2Cl_2 containing 0.1 mol dm^{-3} [NBu_4][ClO_4] at a scan rate of 10 mV s^{-1}.

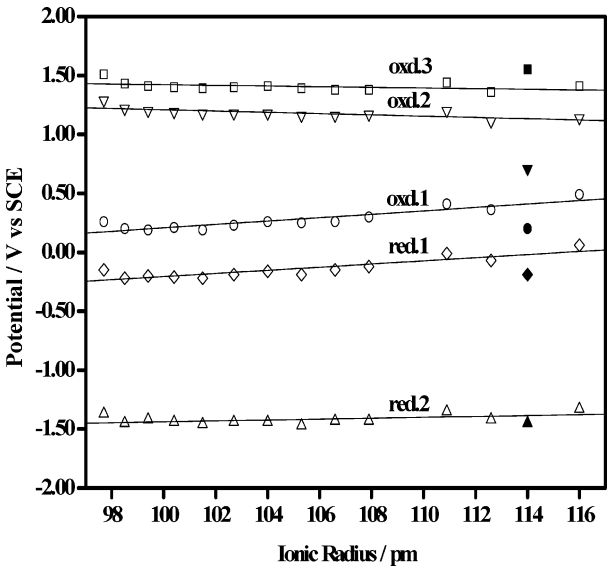

Figure 9. Redox potentials of [M(Nc)(OEP)] (M = Y, La−Lu except Ce and Pm) as a function of the ionic radius of the metal center.[24] The darkened data points represent the corresponding potentials of the cerium analogue **5**.

(37) Zhu, P.; Lu, F.; Pan, N.; Arnold, D. P.; Zhang, S.; Jiang, J., manuscript in preparation.

and +1.83 V for **5** involve a successive removal of electrons from the ligand-based orbitals: $[Ce^{X}(Nc)(OEP)]/[Ce^{X}(Nc)(OEP)]^{+}$, $[Ce^{X}(Nc)(OEP)]^{+}/[Ce^{X}(Nc)(OEP)]^{2+}$, $[Ce^{X}(Nc)(OEP)]^{2+}/[Ce^{X}(Nc)(OEP)]^{3+}$, and $[Ce^{X}(Nc)(OEP)]^{3+}/[Ce^{X}(Nc)(OEP)]^{4+}$, respectively. As shown in Figure 9, the first three oxidation potentials of **5** deviate significantly from the linear relationships found for the other $[M^{III}(Nc)(OEP)]$.[19b] It is clear that the cerium ion in these redox states is not trivalent and may have the same formal charge as in neutral [Ce(Nc)(OEP)]. The electrochemical behavior of **3** and **4** was similar to that of **5** and could be interpreted in a similar manner. The redox potentials of **3**, however, appeared at more positive positions as a result of the less delocalized Pc ligand.

The electrochemical behavior of $[Ce\{Nc(t\text{Bu})_4\}_2]$ (**2**) was reinvestigated.[13] It is remarkably different from that of the other cerium double-deckers **1** and **3**−**5** due to the different valence of the metal center. Four quasi-reversible one-electron oxidations (two more than previously recorded results) and four quasi-reversible one-electron reductions (one more than previously recorded results) were observed under the present improved conditions. The second, third, and fourth reduction couples at −1.20, −1.52, and −1.88 V can be attributed to a successive addition of electrons to the ligand-based orbitals: $[Ce\{Nc(t\text{Bu})_4\}_2]^{-}/[Ce\{Nc(t\text{Bu})_4\}_2]^{2-}$, $[Ce\{Nc(t\text{Bu})_4\}_2]^{2-}/[Ce\{Nc(t\text{Bu})_4\}_2]^{3-}$, and $[Ce\{Nc(t\text{Bu})_4\}_2]^{3-}/[Ce\{Nc(t\text{Bu})_4\}_2]^{4-}$ respectively. The cerium ion in these redox states is trivalent, again because both the second and third reduction potentials follow the trend observed for $[M^{III}\{Nc(t\text{Bu})_4\}_2]$ (M = La, Pr, Nd, Eu, Gd, Tb, Y, Er).[13] Unlike **1** and **3**−**5**, the first reduction and the first oxidation waves at −0.11 and +0.17 V are also ring-centered involving a pure trivalent cerium state: $[Ce^{III}\{Nc(t\text{Bu})_4\}_2]/[Ce^{III}\{Nc(t\text{Bu})_4{}^{2-}\}_2]^{-}$ and $[Ce^{III}\{Nc(t\text{Bu})_4\}_2]/[Ce^{III}\{Nc(t\text{Bu})_4\}_2]^{+}$, respectively, as these redox potentials also fit perfectly into the linear relationships observed for the other $[M^{III}\{Nc(t\text{Bu})_4\}_2]$. The second oxidation process at +0.69 V also seems to be a ring-based oxidation. However, it is likely that the Ce^{III}/Ce^{IV} couple is also embedded at this position (ca. +0.69 V) based on its larger peak to peak separation as shown in its cyclic voltammogram and the slightly split peaks in its differential pulse voltammogram. Further evidence was obtained by chronoamperometric and chronocoulometric studies as described in the Supporting Information. This implies that the trivalent cerium ion and the substituted naphthalocyanine ligand are fortuitously oxidized at very close potentials, similar to what was observed for mixed (phthalocyaninato)(porphyrinato)cerium(III) triple-deckers $[Ce^{III}_2(Pc)(TPP)_2]$ and $[Ce^{III}_2(Pc)_2(TPP)]$.[8f] The third and fourth oxidations at +1.36 and +1.54 V are also ligand-based processes involving the redox states: $[Ce^{X}\{Nc(t\text{Bu})_4\}_2]^{2+}/[Ce^{X}\{Nc(t\text{Bu})_4\}_2]^{3+}$ and $[Ce^{X}\{Nc(t\text{Bu})_4\}_2]^{3+}/[Ce^{X}\{Nc(t\text{Bu})_4\}_2]^{4+}$, respectively, in which the value of *X* lies between III and IV by analogy to the results for **1** and **3**−**5** described above.

Structural Studies. The molecular structures of [Ce(Pc)(TPyP)] (**3**) and [Ce(Nc)(OEP)] (**5**) were determined by X-ray diffraction analyses. The single crystals were grown by slow diffusion of MeOH (for **3**) or hexane (for **5**) into their $CHCl_3$ solutions and it was found that both structures contained solvated species ($CHCl_3$, MeOH, and water in **3** and cyclohexane in **5**). It is likely that the unexpected water and cyclohexane were present as impurities in the solvents we used.[38] Figure 10a shows a perspective view of the structure of **3**, in which the cerium center is octa-coordinated by the isoindole and pyrrole nitrogen atoms of the Pc and TPyP rings, respectively, forming a nearly perfect square antiprism as shown in Figure 10b. The two N_4 mean planes are virtually parallel (dihedral angle = 0.2°) with a plane-to-plane separation of 2.794 Å. The cerium center lies closer to the TPyP N_4 plane (1.340 vs 1.454 Å), probably due to the larger cavity size of TPyP.[39] Like the structures of many double-decker complexes,[1b−d] the two ligands are not planar and display a saucer shape. Table 4 lists some of the structural parameters of **3**, which are comparable with those of [Ce(Pc)(TMPP)].[7,8b]

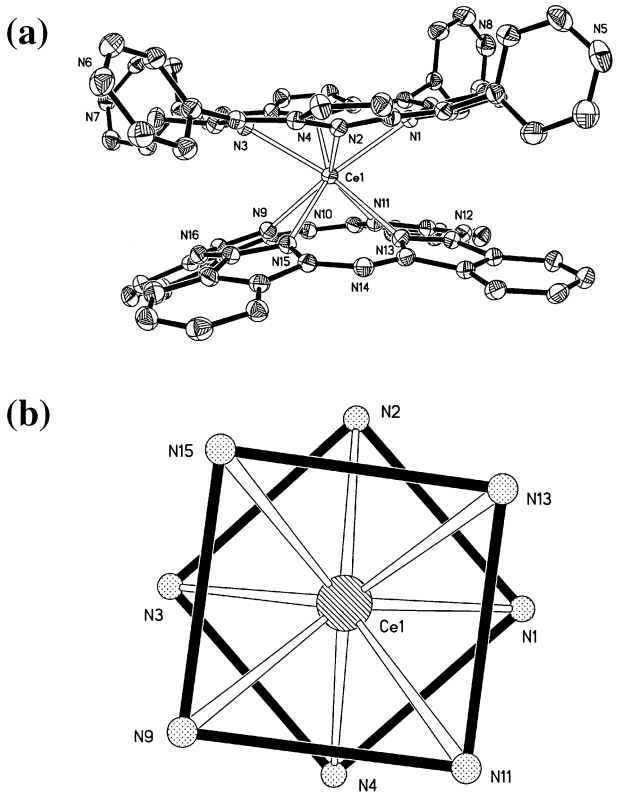

Figure 10. (a) Molecular structure of [Ce(Pc)(TPyP)] (**3**) showing the 30% probability thermal ellipsoids for all non-hydrogen atoms. (b) The square anti-prismatic coordination environment around the cerium center.

The cerium center of compound **5** also adopts a square antiprimatic geometry and the overall structure (Figure 11) resembles those of the other lanthanide analogues $[M^{III}(Nc)(OEP)]$ (M = Y, La, Pr−Lu except Pm)[19,40] It has been found that for this series of complexes, the interplanar separation and the average M−N distances decrease consistently with the size of the metal center. The structural data of **5** (Table 4), however, do not follow this trend. As shown in Figures 4 and 5 in ref 40, the best-fit straight lines are flanked by two hypothetical points generated by taking the ionic radii of cerium(III) and cerium(IV) ions. This also demonstrates the intermediate valence adopted by cerium in this complex.

(38) The presence of ca. 1% cyclohexane in the hexane we used was confirmed by gas chromatography.
(39) Boucher, L. In *Coordination Chemistry of Macrocyclic Compounds*; Melson, G. A., Ed.; Plenum: New York, 1979; pp 465−466.
(40) Bian, Y.; Wang, D.; Wang, R.; Weng, L.; Dou, J.; Zhao, D.; Ng, D. K. P.; Jiang, J. *New J. Chem.* **2003**, *27*, 844.

Table 4. Structural Data for [Ce(Pc)(TPyP)] (**3**) and [Ce(Nc)(OEP)] (**5**)

	3	5
average Ce−N(Pc/Nc) bond distance (Å)	2.457	2.473
average Ce−N(TPyP/OEP) bond distance (Å)	2.462	2.442
Ce−N_4(Pc/Nc) plane distance (Å)	1.454	1.479
Ce−N_4(TPyP/OEP) plane distance (Å)	1.340	1.291
interplanar distance (Å)	2.794	2.770
dihedral angle between the two N_4 planes (°)	0.2	0.4
average dihedral angle ϕ for the Pc/Nc ring (°)[a]	15.1	13.5
average dihedral angle ϕ for the TPyP/OEP ring (°)[a]	12.3	15.0
average twist angle (°)[b]	41.1	45.0
average dihedral angle φ between the pyridyl rings and the TPyP N_4 plane (°)	75.0	

[a] The average dihedral angle of the individual isoindole or pyrrole rings with respect to the corresponding N_4 mean plane. [b] Defined as the rotation angle of one ring away from the eclipsed conformation of the two rings.

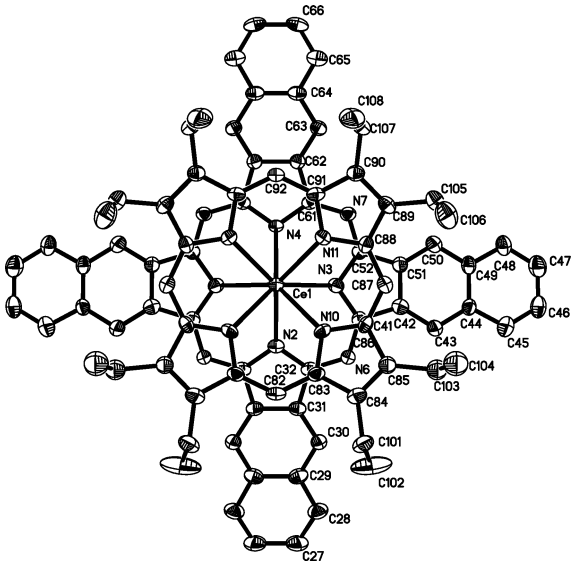

Figure 11. Molecular structure of [Ce(Nc)(OEP)] (**5**) showing the 30% probability thermal ellipsoids for all non-hydrogen atoms.

Conclusion

Among the whole rare earth series, cerium is unique due to its special electronic configuration. In this study, we have employed a range of spectroscopic, electrochemical, and structural methods to elucidate the valence of the cerium center in a series of tetrapyrrole double-decker complexes. Depending on the electronic nature of the π ligands, the cerium center adopts an intermediate valence, ranging from predominantly trivalent (for **2**) to predominantly tetravalent (for **3**−**5**). The results have been supported by XANES studies.

Experimental Section

The details of purification of solvents, preparation of precursors, and spectroscopic measurements have been reported elsewhere.[16b,18,33] The double-deckers **1a**,[14] **1b**,[15] and **2**[13] were prepared as described.

CV and DPV measurements were carried out with a BAS CV-50W voltammetric analyzer. The cell comprised inlets for a glassy carbon disk working electrode and a silver-wire counter electrode. The reference electrode was Ag/Ag^+ connected to the solution by a Luggin capillary whose tip was placed close to the working electrode. Results were corrected for junction potentials by being referenced internally to the ferrocenium/ferrocene (Fe^+/Fe) couple [$E_{1/2}(Fe^+/Fe) = +0.50$ V vs SCE]. Typically, a 0.1 mol dm^{-3} solution of $[NBu_4][ClO_4]$ in CH_2Cl_2 containing 0.5 mmol dm^{-3} of sample was purged with nitrogen for 10 min, then the voltammograms were recorded at ambient temperature. The chronoamperometric and chronocoulometric studies were performed on a BAS 100B/W electrochemical analyzer using a platinum disk working electrode with a diameter of 2 mm.

Preparation of [Ce{Pc($OC_{12}H_{25}$)$_8$}$_2$] (1c). A mixture of $[Ce(acac)_3]\cdot nH_2O$ (22 mg, 0.05 mmol), 4,5-bis(dodecyloxy)phthalonitrile (0.30 g, 0.60 mmol), and DBU (40 mg, 0.26 mmol) in *n*-pentanol (2 mL) was refluxed under a slow stream of nitrogen for 12 h. The mixture was cooled briefly, and the volatiles were removed under reduced pressure. The residue was chromatographed on a silica gel column using $CHCl_3$ as eluent. A green band of the target double-decker was developed followed by a fraction of the metal-free phthalocyanine H_2{Pc-($OC_{12}H_{25}$)$_8$}. The crude product was further purified by repeated chromatography followed by reprecipitation from a mixture of $CHCl_3$ and MeOH. Yield 45 mg (22%); ^{1}H NMR (300 MHz, $CDCl_3$): δ 8.47 (s, 16 H, Pc-H_α), 4.78−4.85 (m, 16 H, OCH_2), 4.45−4.50 (m, 16 H, OCH_2), 2.12−2.27 (m, 32 H, CH_2), 1.75−1.82 (m, 32 H, CH_2), 1.26−1.50 (m, 256 H, CH_2), 0.89 (t, J = 6.6 Hz, 48 H, CH_3); MS (MALDI-TOF): an isotopic cluster peaking at m/z 4114 (M^+); elemental analysis calcd (%) for $C_{261}H_{430}CeCl_6N_{16}O_{19}$ (**1c**·2$CHCl_3$·3MeOH): C 70.46, H 9.74, N 5.04; found: C 70.52, H 10.45, N 4.50.

Preparation of [Ce(Pc)(TPyP)] (3). A mixture of Li_2Pc (125 mg, 0.24 mmol) and $[Ce(acac)_3]\cdot nH_2O$ (100 mg, 0.23 mmol) in TCB (8 mL) was heated at 120 °C for 4 h under a slow stream of nitrogen. The resulting blue solution was cooled briefly, then H_2(TPyP) (62 mg, 0.10 mmol) was added, and the mixture was refluxed for a further 12 h. The solvent was then removed in vacuo, and the residue was chromatographed on a silica gel column using $CHCl_3$ as eluent. A small amount of the blue [Ce(Pc)$_2$] and the green triple-decker [Ce$_2$(Pc)$_2$(TPyP)] (6 mg, 3%) were first obtained. The column was then further eluted with 3% MeOH in $CHCl_3$ to give green fractions of the double-decker [Ce(Pc)(TPyP)] (**3**) (88 mg, 69%) and the triple-decker [Ce$_2$(Pc)(TPyP)$_2$] (18 mg, 18%). The major product **3** was further purified by the same chromatographic procedure followed by recrystallization from a mixture of $CHCl_3$ and MeOH. ^{1}H NMR (300 MHz, $CDCl_3$): δ 9.20 (dd, J = 3.0, 5.7 Hz, 8 H, Pc-H_α), 8.98 (br. s, 4 H, C_6H_4N), 8.50 (br. s, 4 H, C_6H_4N), 8.32 (s, 8 H, TPyP−H_β), 8.26 (dd, J = 3.0, 5.7 Hz, 8 H, Pc-H_α), 7.13 (br. s, 4 H, C_6H_4N), 6.40 (br. s, 4 H, C_6H_4N); MS (MALDI-TOF): an isotopic cluster peaking at m/z 1270 (M^+); elemental analysis calcd (%) for $C_{73.5}H_{41.5}CeCl_{4.5}N_{16}$ (**3**·1.5$CHCl_3$): C 60.95, H 2.89, N 15.47; found: C 60.88, H 2.56, N 15.24.

Preparation of [Ce(Nc)(TBPP)] (4) and [Ce(Nc)(OEP)] (5). A mixture of $[Ce(acac)_3]\cdot nH_2O$ (44 mg, 0.10 mmol), H_2(Por) (Por = TBPP, OEP) (0.05 mmol), naphthalonitrile (72 mg, 0.40 mmol), and DBU (50 mg, 0.33 mmol) in *n*-octanol (4 mL) was refluxed overnight (>18 h) under nitrogen to give a dark-green solution. The volatiles were removed under reduced pressure and the residue was chromatographed on a silica gel column with CH_2Cl_2/hexane (1:1, v/v) as eluent to remove the unreacted metal-free porphyrin. The column was further eluted successively with CH_2Cl_2, $CHCl_3$, and MeOH in $CHCl_3$ (3%) to give a blue band containing the desired double-decker. The crude product was further purified by the same chromatographic procedure followed by recrystallization from a mixture of $CHCl_3$ and MeOH to

Table 5. Crystallographic Data for [Ce(Pc)(TPyP)] (**3**) and [Ce(Nc)(OEP)] (**5**)

	3•$CHCl_3$•0.5MeOH•0.5H_2O	**5**•0.5C_6H_{12}
formula	$C_{73.5}H_{44}CeCl_3N_{16}O$	$C_{87}H_{74}CeN_{12}$
M_r	1413.7	1427.7
crystal size [mm^3]	0.30 × 0.18 × 0.18	0.32 × 0.30 × 0.08
crystal system	triclinic	orthorhombic
space group	P_{1-}	*Pnam*
a [Å]	12.889 (3)	29.048 (7)
b [Å]	13.984 (3)	10.888 (2)
c [Å]	18.305 (4)	26.642 (6)
α [°]	95.64 (3)	90
β [°]	105.44 (3)	90
γ [°]	98.36 (3)	90
V [$Å^3$]	3113.8 (11)	8426 (3)
Z	2	4
F(000)	1428	2952
ρ_{calcd} [$Mg\ m^{-3}$]	1.508	1.125
μ [mm^{-1}]	0.922	0.588
θ range [°]	1.74 to 25.53	1.60 to 24.00
reflections collected	9842	40613
independent reflections	9801 (R_{int} = 0.0000)	6780 (R_{int} = 0.1634)
parameters	866	445
*R*1 [$I > 2\sigma(I)$]	0.0577	0.0740
w*R*2 [$I > 2\sigma(I)$]	0.1724	0.2022
goodness of fit	1.214	1.063

give dark blue microcrystals. **4**: Yield 14 mg (17%); ^{1}H NMR (300 MHz, $CDCl_3$): *δ* 6.88 (br. s, 4 H, C_6H_4tBu), 6.81 (br. s, 4 H, C_6H_4tBu), 6.10 (br. s, 8 H, Nc-H_β), 5.72 (br. s, 8 H, TBPP−H_β), 5.67 (br. s, 4 H, C_6H_4tBu), 5.15 (br. s, 8 H, Nc-H_γ), 4.46 (br. s, 4 H, C_6H_4tBu), 1.10 (s, 27 H, *t*Bu); MS (MALDI-TOF): an isotopic cluster peaking at *m*/*z* 1690 (M^+); elemental analysis calcd (%) for $C_{108}H_{84}CeN_{12}$: C 76.75, H 5.01, N 9.95; found: C 76.69, H 5.48, N 8.67. **5**: Yield 15 mg (22%); ^{1}H NMR (300 MHz, $CDCl_3$): *δ* 9.40 (br. s, 8 H, Nc-H_α), 8.98 (s, 4 H, *meso*-H), 8.63−8.66 (m, 8 H, Nc-H_β), 7.86−7.89 (m, 8 H, Nc-H_γ), 1.72 (t, *J* = 7.5 Hz, 24 H, CH_3); MS (MALDI-TOF): an isotopic cluster peaking at *m*/*z* 1385 (M^+); elemental analysis calcd (%) for $C_{88}H_{75}CeCl_3N_{12}$ (**5**•0.5C_6H_{12}•$CHCl_3$): C 68.32, H 4.89, N 10.86; found: C 68.70, H 5.45, N 10.68.

X-ray Crystallographic Analyses of [Ce(Pc)(TPyP)] (3) and [Ce(Nc)(OEP)] (5). Crystal data and data processing parameters are given in Table 5. Data collection for **3** was performed at 294 K on a MSC/Rigaku RAXIS IIc imaging-plate system using Mo−Kα radiation (*λ* = 0.710 73 Å) from a Rigaku RU-200 rotating-anode generator operating at 50 kV and 90 mA.[41] A self-consistent semiempirical absorption correction based on Fourier coefficient fitting of symmetry-equivalent reflections was applied by using the ABSCOR program.[42] The structure was solved by direct methods, which yielded the positions of all non-hydrogen atoms, which were refined anisotropically. Hydrogen atoms were placed in their idealized positions (C−H 0.96 Å) with fixed isotropic thermal parameters and allowed to ride on their parent carbon atoms. All the H atoms were held stationary and included in structure factor calculations in the final stage of full-matrix least-squares refinement. All computations were performed with a PC computer using the SHELX-97 program package.[43]

For compound **5**, the data were collected on a Bruker SMART CCD diffractometer with an Mo−Kα sealed tube (*λ* = 0.710 73 Å) at 293 K, and by using a *ω* scan mode with an increment of 0.3°. Preliminary unit cell parameters were obtained from 45 frames. Final unit cell parameters were derived by global refinements of reflections obtained from integration of all the frame data. The collected frames were integrated by using the preliminary cell-orientation matrix. SMART software was used for collecting frames of data, indexing reflections, and determination of lattice constants; SAINT-PLUS for integration of intensity of reflections and scaling;[44] SADABS for absorption correction;[45] and SHELXL for space group and structure determination, refinements, graphics, and structure reporting.[46]

X-ray Absorption Near-Edge Structure (XANES) Measurements. XANES spectra were collected on beamline 4W1B at the Beijing Synchrotron Radiation Facilities (BSRF) in the Institute of High Energy Physics, Chinese Academy of Sciences. The intensity of X-ray was adjusted to decrease by 40% to eliminate harmonic. The X-ray white light from 2.2-GeV electron storage ring was monochromatized by an Si(111) double crystal monochromator, which yields a resolution of approximately 1.5 eV at 6 keV. The storage ring current was between 60 and 100 mA during the measurements. Calibration of the energy was made using [CeO_2] as standard. XANES spectra were collected at the cerium L_{III}-edge and all the measurements were in transmission mode. After removing the pre-edge background, the XANES data were normalized to a unit edge jump for comparison. The cerium complexes [$Ce(NO_3)_3$•$6H_2O$] and [CeO_2] were used as references.

Acknowledgment. We thank Profs. K.-K. Shiu and Nagao Kobayashi for advice and technical assistance in the chronoamperometric and chronocoulometric measurements. Financial support from the Natural Science Foundation of China (Grant No. 20171028), the National Ministry of Science and Technology of China (Grant No. 2001CB6105-04), the National Ministry of Education of China, the Natural Science Foundation of Shandong Province (Grant No. Z99B03), the Science Committee of Shandong Province, Shandong University, Queensland University of Technology, and The Chinese University of Hong Kong is gratefully acknowledged.

Supporting Information Available: Plot of wavenumbers of the *π*-radical anion band, Q-band, and the longest-wavelength near-IR band of [M{Nc(*t*Bu)$_4$}$_2$] as a function of the ionic radius of the M^{III} ions (Figure S1), plot of wavenumbers of the two Q-bands of [M{Nc(*t*Bu)$_4$}$_2$]$^-$ as a function of the ionic radius of the M^{III} ions (Figure S2), Ce L_{III} absorption threshold of [Ce(Nc)(OEP)] (**5**) after subtraction of an arctangent curve and the results of fitting with three Lorentzian functions (Figure S3), chronoamperometric and chronocoulometric data of [Ce{Nc(*t*Bu)$_4$}$_2$] (**2**) (Figure S4), and complete crystallographic details of the X-ray structures of **3** and **5** (PDF and CIF). This material is available free of charge via the Internet at http://pubs.acs.org.

JA036017+

(41) (a) Tanner, J.; Krause, K. *Rigaku J.* **1994**, *11*, 4. (b) Tanner, J.; Krause, K. *Rigaku J.* **1990**, *7*, 28. (c) Krause, K. L.; Phillips, Jr. G. N. *J. Appl. Crystallogr.* **1992**, *25*, 146. (d) Sato, M.; Yamamoto, M.; Imada, K.; Katsube, Y.; Tanaka, N.; Higashi, T. *J. Appl. Crystallogr.* **1992**, *25*, 348.
(42) Higashi, T. *ABSCOR—An Empirical Absorption Correction Based on Fourier Coefficient Fitting*, Rigaku Corporation, Tokyo, 1995.
(43) Sheldrick, G. M. *SHELX-97: Package for Crystal Structure Solution and Refinement*, University of Göttingen, Germany, 1997.
(44) *SMART and SAINT for Windows NT Software Reference Manuals*, Version 5.0, Bruker Analytical X-ray Systems, Madison, WI, 1997.
(45) Sheldrick, G. M. *SADABS—A Software for Empirical Absorption Correction*, University of Göttingen, Germany, 1997.
(46) *SHELXL Reference Manual*, Version 5.1, Bruker Analytical X-ray Systems, Madison, WI, 1997.